

S.H.A. ALFATLAWI<sup>1\*</sup>, N.M. KHABOU<sup>2</sup>, W.A. MUGHIR<sup>1</sup>

## EVALUATE THE ADVANCED MACHINING ON METAL MATRIX COMPOSITE MANUFACTURED VIA ADDING NANO-ALUMINUM OXIDE ON RECYCLED ALUMINUM WASTE

A waste of electrical power cables becomes a major problem at the present time, so they must be disposed in order to preserve the environment, and to obtain a raw material for the industry with low cost. In this work, recycled materials is prepared by heating up the aluminum wires up to 650°C for melting to prepare the aluminum alloy as a matrix. Then, the matrix reinforced by the nanoparticles (30 nm) of aluminum oxide (Al<sub>2</sub>O<sub>3</sub>) to prepare the composite using the stir casting technique. The electrical discharge machining (EDM) as advanced machining, is used to evaluate the materials behavior through the operation. Taguchi method is used to design and determine the suitable input and output factors. The scanning electron microscope (SEM) and hardness are tested before and after machining. The results appeared that improving in microstructure, also the hardness of the composite improved (37.2% and 22.6%) before and after machining.

*Keyword:* Aluminum wire recycling; Nano-aluminum oxide; Stir casting; Scanning electron microscope (SEM); Electrical discharge machine (EDM)

### 1. Introduction

The optimization of aluminum and its alloys properties, such as good conductivity of electricity and heat, light weight corrosion resistant etc., led to wide applications. Therefore, it is used in land, sea, and air transportation, communications, etc., thus too many applications cause waste and scraps that must be disposed of. In addition, there are many methods for aluminum manufacturing, such as stir casting, powder metallurgy, and various pressure castings [1,2].

Mostly, aluminum recycling is accompanied continuous innovations to overcome difficulties, the most important which is the impurities associated with the melting process. Therefore, the interest was treated this problem by improving the melting process using downgrading and dilution techniques. As well as, other modern methods for scrap separating, such as high-pressure of jetting water. Other methods, such as 3D cameras and concentration analysis, contribute to proper sorting of scrap. Thus, dealing with scrap, such as sorting, cutting, and deposits removing, which increases the efficiency of the process. Furthermore, melting furnace choice depends on the quantity and quality of scrap, that with the highest melting per unit volume at reducing cost and time [3,4].

Stir casting is used to manufacture aluminum-based composite materials due to its distinctive properties, such as using easy, good mixing, and cheap. Moreover, the products of this method are characterized by acceptable porosity and density and good mechanical properties [5]. Therefore, the features of particle-reinforced aluminum matrix composites, that makes it ideal for aerospace, automotive, underwater and transportation applications. Hence, the manufacturing process is very important, that mean the stir casting factors such as pouring temperature, stirring and material quality are maintained. There are other techniques for manufacturing aluminum matrix composite, such as, vapor deposition, diffusion bonding, powder metallurgy and friction stir, etc. [6,7].

Consequently, alumina (Al<sub>2</sub>O<sub>3</sub>) has several phases, including alpha, gamma, beta, and delta, depending on the manufacturing temperature. The alpha phase is used more widely, because its high density compared to other phases. Alumina has many applications due to its distinctive properties, such as high wear resistance, strength and hardness. As well as, corrosion resistance, good resistance of chemical, high point of melting and thermal stability. There are several methods for alumina manufacturing, each method has advantages and disadvantages. These, including precipitation, wet chemical, soil-gel, combustion and

<sup>1</sup> UNIVERSITY OF BABYLON, COLLEGE OF MATERIAL'S ENGINEERING, IRAQ

<sup>2</sup> UNIVERSITY OF SFAX, ELECTROMECHANICAL SYSTEMS LABORATORY (LASEM), NATIONAL ENGINEERING SCHOOL OF SFAX, BP 1173 3038 SFAX, TUNISIA

\* Corresponding author: [mat.sattar.h@uobabylon.edu.iq](mailto:mat.sattar.h@uobabylon.edu.iq)



microwave, etc. The best method is precipitation, because it's easy, cheap, less pollution, thermal stability, high purity, and homogeneity size [8,9]. Aluminum matrix composite meets the needs of development, so it is used in the field of aviation, aerospace and transportation in general. It has low density, wear resistance, strength and stiffness, good flexible preparation and heat treatment, and good conductivity of electric and heat [10].

Recently, many studies have been conducted to develop the aluminum matrix in order to reinforce it with different materials depending on the type of application. Also, the mechanical behavior, tribology of surface and lubricated sliding conditions was studied to reduce the friction and wear [11,12]. Also, stir casting method is used to manufacture aluminum alloy, that reinforced by carbon nanotubes. Thus, the results are shown grain size is reduced, as well improved the corrosion behavior and sliding wear [13]. Likewise, the cyclic extrusion compression method is used to improve the hardness and corrosion behavior of aluminum alloy (Al5052), also evaluate the microstructure of aluminum alloy [14].

The stir casting method is suitable for aluminum matrix composite, because it contributes to uniform distribution of reinforcement particles. This is achieved by increasing the mixing time of the titanium boride ( $TiB_2$ ) particles in the aluminum matrix. As well as, aluminum matrix composites can be improved by silicon carbide (SiC), that prepared by the stir casting method. The improvements of microstructure, hardness and strength of compressive, are achieved [15,16]. In this regard, the stir casting is used to prepare an aluminum matrix reinforced with  $Al_2O_3$  at 6% and 8% weight to manufacture aluminum matrix composite. Then, the specimen is machined by wire electric discharge machining (WEDM). Therefore, better results material removal rate (MRR) and roughness (Ra) with 6 weight% additives [17]. Aluminum matrix composite produced by stir casting reinforced with 4% tungsten carbide. Grey regression analysis was used to estimate the main input factors for the EDM process [18].

Furthermore, EDM is used in the processing of aluminum matrix reinforced with different percentages of silicon carbide. Then use analysis of variance (ANOVA) to reach of the output characteristics of the material machined by EDM [19]. The machining behavior of aluminum matrix reinforced with  $Al_2O_3$  and SiC, that prepared by stir casting was analyzed. The procedure was to change the input parameters to three levels according to Taguchi design. The outputs parameters of the three levels were evaluated, and then analysis of variance (ANOVA) was performed to determine the most influential [20].

Previous literature indicated that the stir casting method is the appropriate method to manufacture aluminum matrix composite reinforced with advanced ceramic materials. In the current work, the aluminum matrix composite is prepared from recycled aluminum cable scrap with nano-alumina particles ( $Al_2O_3$ ) as strengthening materials. The work aims are; to use a recycled raw materials represented by scrape aluminum wires. In addition, provide corrosion resistance. Furthermore, lightweight composite materials can be obtained, as well as the EDM will be used to evaluate the effect of operating conditions on the manufactured materials.

## 2. Experimental procedure

### 2.1. Materials preparation

In the current work, the aluminum wire scrap that used to transmit the electrical energy is recycled to prepare aluminum matrix, which has lowest hardness compared to  $Al_2O_3$ . Thus, there is no need to a modern recycling process, in other words, do not need a complex sorting process to rid the impurities. Because the aluminum wire scrap, do not include many impurities. The required amount of aluminum wire scrap ( $\varnothing 2$  mm) was cleaned of dirt, and cut into 20 mm length of pieces. It is then placed inside the furnace to make the matrix after melting, so adding the magnesium strip. Magnesium is added to improve wettability and increase cohesion between the matrix and the reinforcement. The chromium powder is added to improve the corrosion resistant. In addition, the reinforcements particle of alpha nano-alumina ( $\alpha$ -nano- $Al_2O_3$ ) with size (30 nm) is prepared, that is used to improve the aluminum matrix composite. As well as, all instruments prepared such as furnaces, stir casting and testes, mold, and EDM machine.

### 2.2. Samples casting

The pieces of aluminum wire were placed on the graphite crucible inside the furnace, then the temperature was slowly raised until settled at  $650^\circ C$ , the slag floats on the molten should be removed. The electric mixer at a speed (750 rpm) is used for mixing the molten materials. Thus, the magnesium and chromium wrap in aluminum foil and heated at  $150^\circ C$ , then placed in a melting pot at (2.5 wt.%) and (0.25 wt.%) respectively. The aqueous aluminum chloride is added to the molten as an aid to slag removal, that continues removing of the slag. Furthermore, molten is good mixing at pouring temperature, the crucible is lifted outside the furnace, the molten was poured into a preheated mold, that was heated at ( $250^\circ C$ ).

Then, the mold is filled with molten and left until cooled at room temperature to get the alloy sample (AA5052). Sequentially, the particles of ( $\alpha$ -nano-  $Al_2O_3$ ) at (6. wt.%), is covered with aluminum foil and heating at ( $150^\circ C$ ). The previous steps for alloy producing are repeated until the contents dissolve. Then, the temperature is raised to ( $800^\circ C$ ), the preheated  $Al_2O_3$  are added into the molten vortex with continuous stirring. The molten is poured into the mold, sample of (AA5052+  $Al_2O_3$ ) is performed after leaving to cool at room temperature. The process followed by a thermal homogenization to improve the microstructure, that at  $500^\circ C$  before conducting the necessary tests.

### 2.3. Samples tests

Samples are prepared for testing in different dimensions depending on the type of test. Samples surface test is prepared by grinding and polishing the surface by emery papers (100, 300,

500, 700, 900, 1000), then etching. Thus, the solution (2%HF, 3%HCL, and 5% HNO<sub>3</sub>) are used to conduct the etching processes before SEM test. The SEM test is achieved by (Thermo scientific- Axia) before and after machining, to check the effect of added strengthening materials on the structure of the composite material. The hardness test is conducted by device (Wilson Hardness/ REICHERTER UH250) with a Brinell method at of a ball diameter (2.5 mm), (31.25 Kg) force and (10 sec) of time.

## 2.4. Electric discharge machining procedures

EDM is used in certain circumstances, such as the difficulty of operating with traditional methods, as well as obtaining high operating accuracy. The surfaces of composite material sample are machined by electric discharge machine (CHMER 50 N), the input parameters of machining are selected. That, depending on the previous studies and design by orthogonal array (L9) of Taguchi process is used in the design. The orthogonal array manages the level and configuration of process-affecting control parameters. It is advised to apply the Taguchi approach in order to minimize the quantity of trials conducted. Moreover, three input parameters with three levels of the operations are listed in (TABLE 1), these peak currents ( $I_p$ ), pulse-on time ( $T_{on}$ ) and pulse-off time ( $T_{off}$ ) are selected.

TABLE 1  
Output parameters with their level

Parameters	$I_p$ (A)	$T_{on}$ ( $\mu$ s)	$T_{off}$ ( $\mu$ s)
Level 1	12	50	25
Level 2	16	100	50
Level 3	20	150	75

As well as, the output factors, which are rate of material removal (MRR), wear rate of tool (TWR), and machining time (MT) of each operation is identified. The tool (copper electrode) has 8.9 g/cm<sup>3</sup> density, and 1cm diameter with 10 cm long is used, also the density of workpieces is achieved by Archimedes method, that was 2.682 g/cm<sup>3</sup>. The cylindrical samples are cut by lathe machine at diameter 13 mm and 6mm height. So, the output factors and levels designed by Taguchi method, and the results of three output factors, these are listed in TABLE 2.

Furthermore, the workpiece and the tool are weighed before and after the operations, then the input factors ( $I_p$ ,  $T_{on}$  and  $T_{off}$ ) are entered into the machine. Thus, at the end of each operation, the time is recorded from machine, the tool and the workpiece are re-weighed after the end of each operation to compute the difference in weight. Then, the previous steps are repeated for each operation of the nine trials.

$$\text{MRR} = \frac{w_i - w_f}{\rho \cdot T} \quad (1)$$

$$\text{TWR} = \frac{w_i - w_f}{\rho \cdot T} \quad (2)$$

The Eqs. (1) and (2) are used to calculate the (MRR) of sample, and (TWR) respectively, that for each operation. The  $w_i$  and  $w_f$  represented the weight of samples and the tool before and after the machining, so the ( $\rho$ ) is the density of sample and tool, and ( $T$ ) the time of operation.

TABLE 2  
Experimental parameters and results of Aluminum alloy (AA5052) reinforced by Alumina (Al<sub>2</sub>O<sub>3</sub>)

Exp. No.	$I_p$ (A)	$T_{on}$ ( $\mu$ s)	$T_{off}$ ( $\mu$ s)	Time (min)	MRR (mm <sup>3</sup> /min)	TWR (mm <sup>3</sup> /min)
1	12	50	25	10.15	10.9550	0.0454
2	12	100	50	12.48	10.6050	0.0324
3	12	150	75	12.49	10.2470	0.0275
4	16	50	50	9.42	13.0795	0.0489
5	16	100	75	9.31	13.0537	0.0875
6	16	150	25	5.58	21.1777	0.0946
7	20	50	75	10.04	11.7069	0.0985
8	20	100	25	4.40	28.2904	0.0562
9	20	150	50	5.30	23.5396	0.0445

## 3. Results and Discussion

### 3.1. Microstructure

Usually, melting of aluminum occurs when the temperature rises above the melting point ( $T_m$ ), it turns into the liquid phase. While, during the temperature falls below ( $T_m$ ), the solidification occurs when release the heat of fusion, and the nucleation process begins. That, due to the presence of more sites of heterogeneous nucleation's such as surfaces, grain boundaries, inclusion, etc. Then, After completing nucleates, grain growth continues to complete the crystallization. Thus, magnesium addition is helped in wet ability, and adhesion between the granules. Fig. 1(a and b) shows the images of microstructure test by scanning electron microscopy (SEM) at (1300X) before machining. These, for the samples of alloy (AA5052), and the samples with the addition of nano- Al<sub>2</sub>O<sub>3</sub> particles. Fig. 1a. it is appear the alpha phase of the alloy is clearly visible in the microstructure, with long dendritic shapes and equiaxed grains inside larger grains. Fig. 1b. Shows the image of SEM of alloy reinforced by 6% Al<sub>2</sub>O<sub>3</sub>, that refers to grain growth. Since the nano-alumina particles were deposited on the grain boundaries of the matrix, it seems clear in the SEM image that the grains were equiaxial. Furthermore, a good mixing and adding magnesium to increase adhesion and wettability, were helped to reduce segregation and black spots.

While, the dendrite arms and the grains are smaller if compared with the state of Fig. 1a, in addition, the number of a new arms of dendrite is increased. Hence, the nanoparticles number of alumina increased between the arms of dendrite. Also, the nano-alumina particles have good distribution between the arms of dendrite, and on the boundaries of alloy grains. The nano-alumina particle refinement effect lead to increase in the nuclei number as well as the embryos number. Thus, which leads to improve

the microstructure of the composite material, as it appears clear through increasing the number of secondary dendritic arms. Mostly, the stir casting method is suitable for manufacturing aluminum matrix composites, due to is easy, economical, has the best distribution and reducing agglomerations. While, hardness improves at the expense of ductility, and sometimes there are agglomerations or black spots, that during poor mixing, or difference in density [21,22]. Generally, the structure of castings is improved by homogeneous distribution, good bonding of grains and reduced porosity [23].

Fig. 2(a and b) shows the images of the test by scanning electron microscopy (SEM) at (500×) after machining with best values design of input parameters at highest MRR, that's evident in (TABLE 2). The best values of the input factors with the highest MRR value were chosen, due to the a lot of vibrations of the machine at this value.

That, cause cracks and the appearance of casting defects with the highest MRR (28.2904 mm<sup>3</sup>/min). Thus, these experimental values (20A, 100 μs and 25 μs) of ( $I_p$ ,  $T_{on}$  and  $T_{off}$ ) respectively, refer to clear difference between the figures. The

machining surface of Fig. 2b. Is homogeneous more than that of Fig. 2a, that due to the improvement of the microstructure after reinforced with Al<sub>2</sub>O<sub>3</sub>. In addition, the homogeneous distribution of the reinforcements leads to surface free of cracks after operation, indicates structural cohesion.

### 3.2. Hardness

Fig. 3 shows the hardness test before and after machining, for the samples without and with addition of nanoparticles of (Al<sub>2</sub>O<sub>3</sub>). The values of (a and b) were 62.6 HB and 85.9 HB for Al5052 alloy and composite (Al5052+Al<sub>2</sub>O<sub>3</sub>) before machining, respectively. It is clear that addition effect of (Al<sub>2</sub>O<sub>3</sub>) nanoparticles to aluminum alloy (Al5052), lead to increase the samples hardness. The composite hardness is higher than the samples hardness without the reinforcement particles about 37.2%. That is due to the alumina nanoparticles presence in composite microstructure, that lead to refining the grains of composite. Hence, the nanoparticles of alumina lead to restrict the dislocation

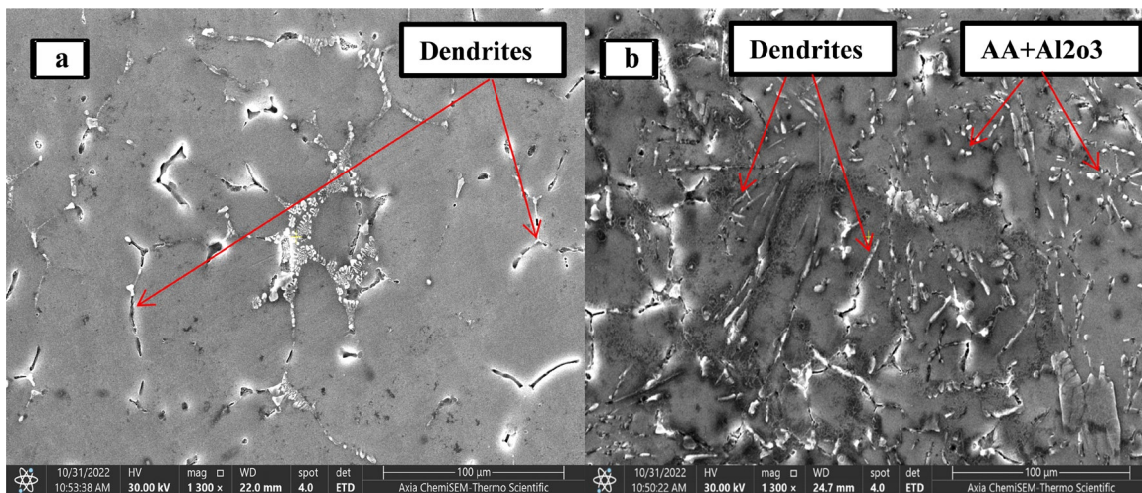


Fig. 1. SEM images before machining, (a) AA5052 image, (b) AA5052+ Alumina

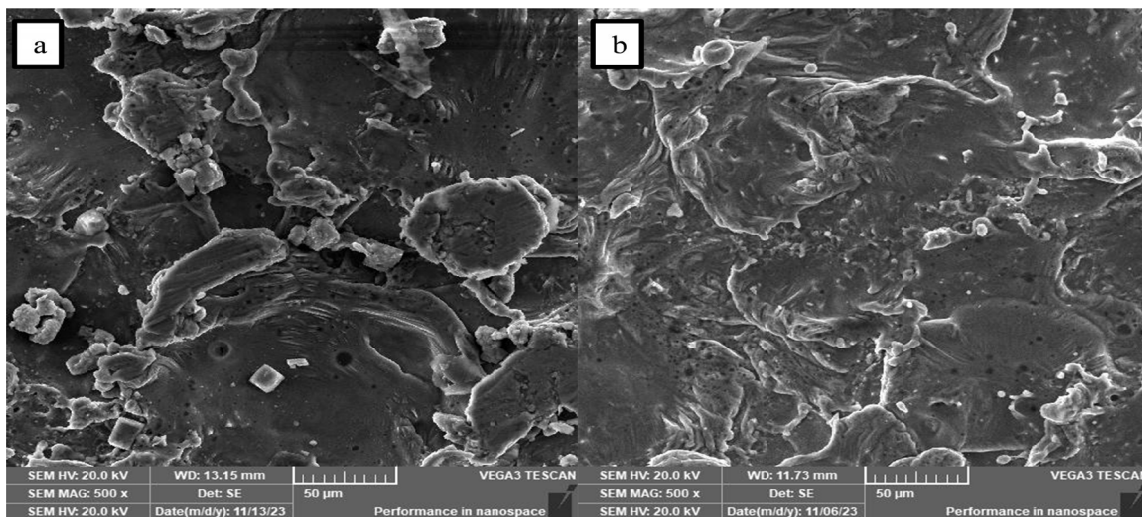


Fig. 2. SEM images after machining with best values design of ( $I_p$ ,  $T_{on}$  and  $T_{off}$ ) for MRR, (a) Al5052 image, (b) Al5052+ Alumina image

movement through checking the samples hardness. Moreover, the nanoparticles ( $Al_2O_3$ ) presence causes high resistance to load, that because the hardness of nanoparticles ( $Al_2O_3$ ). Therefore, the effect of ( $Al_2O_3$ ) causing increasing the dendrite arms, that leads to reduce the crystal size of the structure, seen in Fig. 1b.

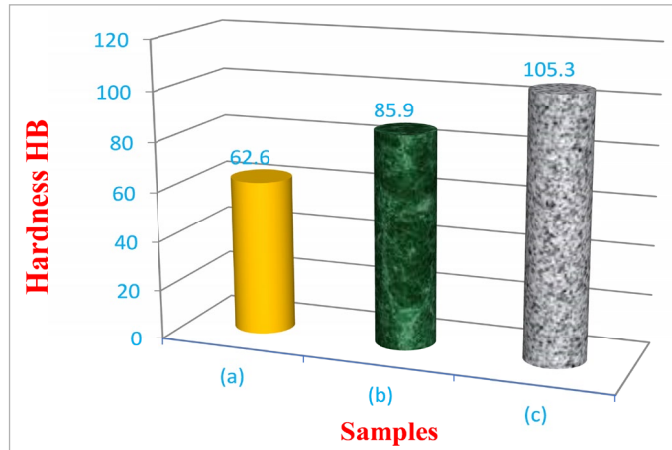


Fig. 3. Hardness of samples with and without the reinforcement, (a) Al5052, (b) Al5052+Al<sub>2</sub>O<sub>3</sub> before machining, (c) Al5052+Al<sub>2</sub>O<sub>3</sub> after machining

Fig. 3c shows the hardness result of composite sample (Al5052+Al<sub>2</sub>O<sub>3</sub>) after machining. Can be seen the effect of surface machining, that lead to increase the hardness into (105.3 HB) due to the change of microstructure. In other word, the sample is subjected under generated heat from electrode spark, then it is cooled by dielectric fluid. Thus, the quenching process leads to hardening the surface concurrently. Therefore, value of composite hardness after machining is higher than the hardness before machining about 22.6%. The current increase of EDM lead to make white layer that has hardness more than the parent metal, then improved the surface hardness [24].

### 3.3. Electric Discharge Machining (EDM)

The machining of electrical discharge was chosen to obtain the high dimensional accuracy and study the effect of additives on machining performance. Also, the cracks occur after machining on the surface or no, that was the main goal of the current study. Therefore, when evaluating the results of the work and obtaining the possible greatest of materials removal rate MRR. In addition, less wear rate of the tool, the shortest period of

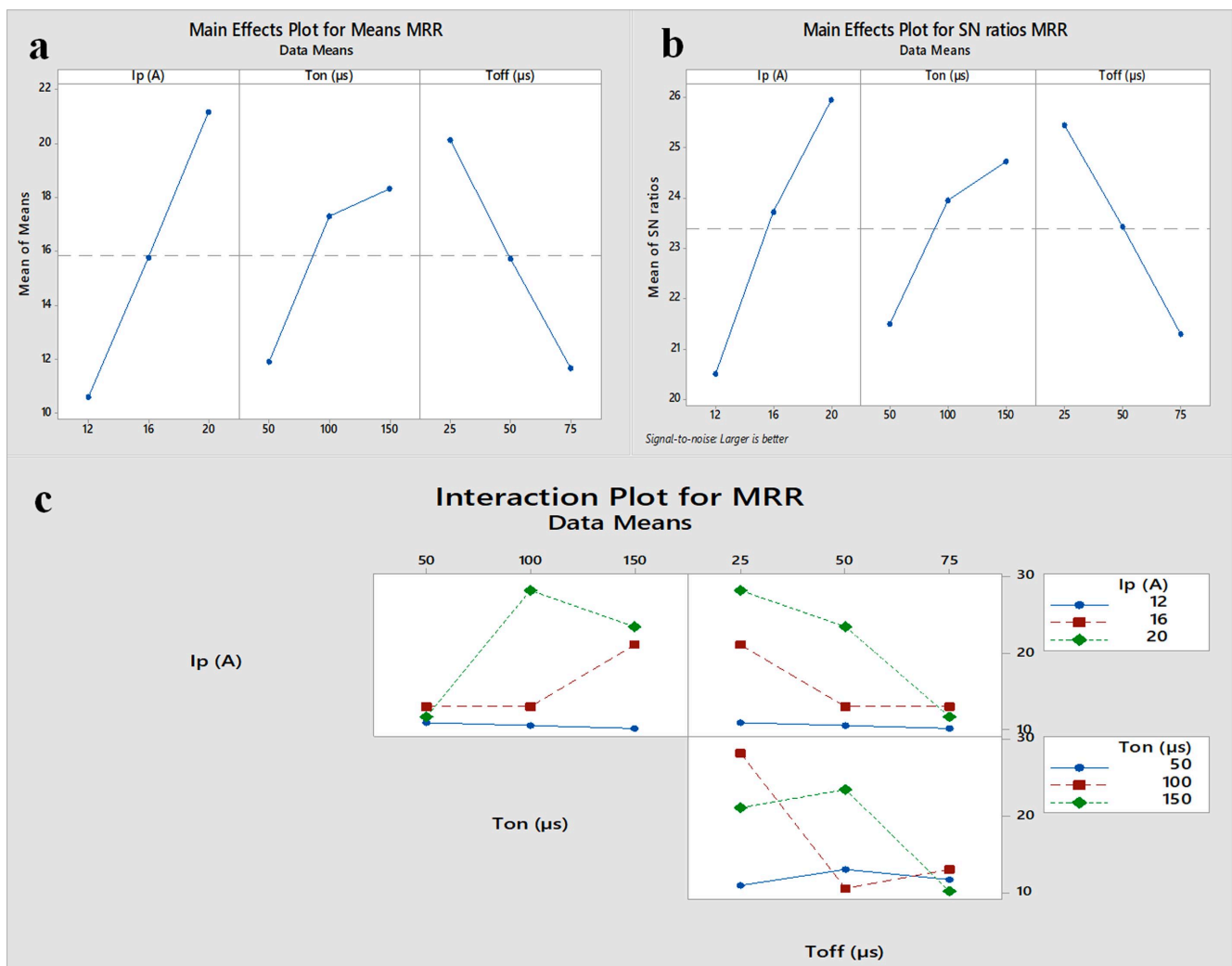


Fig. 4. (a) Main effects plot for Means MRR, (b) Main effects plot (Signal-to-Noise ratio) for MRR, (c) Interaction Plot for MRR Data Means

machining time, and no surface cracks, the goals have been achieved. The appropriate input factors for aluminum alloys and their composite were chosen based on previous studies and design of Minitab software.

Fig. 4a and TABLE 2, appear the MRR increasing, due to increase of  $I_p$ , as does the  $T_{on}$ , continuously. This is due to the ability to melt and vaporize the surface grain increases with increasing  $I_p$  and  $T_{on}$ . That's because the high spark of discharge energy, so the rate of vaporization increases. While, as the  $T_{off}$  increases, the MRR begins to decrease, meaning that it has a negative effect on it. Therefore, the same effects of  $I_p$ ,  $T_{on}$  and  $T_{off}$ , that's clear in fig. 4b, for plot of main effects (Signal-to-Noise ratio) of MRR. The desired goal of this work is to measure the S/N ratio for time (TM) and TWR uses smaller is better and larger is better is used for MRR. Consequently, the raw data is transformed using the smaller is better kind of S/N ratios Eq. (3) and the larger is better kind Eq. (4), which are defined below

$$(S/N)_{\text{Smaller is better}} \text{ ratio} = -10 \log \frac{1}{n} \sum_{i=1}^n y_i^2 \quad (3)$$

$$(S/N)_{\text{Larger is better}} \text{ ratio} = -10 \log \frac{1}{n} \sum_{i=1}^n \frac{1}{y_i^2} \quad (4)$$

To analyze the parameter effect on output response, the optimization of single objective response is used, that with the

largest of MRR and smallest of TWR and machining time (TM). The results of the responses the S/N ratio (Signal-to-Noise ratio) of MRR, TWR and TM are presented in Figs. 4b, 5b and 6b respectively.

Fig. 4c, refers to the interaction influence of process variables on MRR. The interaction effect of input factors, that can be seen during three levels for highest value of MRR. Therefore, the highest value of MRR in level (1), is at 12 A and 50  $\mu$ s of  $I_p$  and  $T_{on}$  respectively. As well as, highest value of MRR is at 16 A and 150  $\mu$ s of  $I_p$  and  $T_{on}$  at level 2, and 20 A and 100  $\mu$ s of  $I_p$  and  $T_{on}$  in level 3. While, highest value of MRR in three levels is achieved at (25, 25 and 50  $\mu$ s) of  $T_{off}$ , that mean the  $T_{off}$  has a negative effect on MRR. Furthermore, the max. value of MRR at (20 A, 100  $\mu$ s and 25  $\mu$ s) of ( $I_p$ ,  $T_{on}$  and  $T_{off}$ ) respectively, can see that in TABLE 2.

Figs. 5(a, b and c), appear the effect of input parameters ( $I_p$ ,  $T_{on}$  and  $T_{off}$ ) on tool wear rate TWR. Figs. 5(a and b) showed the TWR increases due to increases of peak current, that due to the intensity increases of the energy spark. Thus TWR is increased due to its exposure to the continuous spark, which causes the melting of tool tip grains. After that, the TWR begins to decrease as the current increases, due to the increase in the pulse-on time. Which has a positive effect on TWR, especially with the pulse-on time increasing, the TWR decreases. But with the  $T_{off}$ , the TWR decreases and then begins to increase in case of increased current.

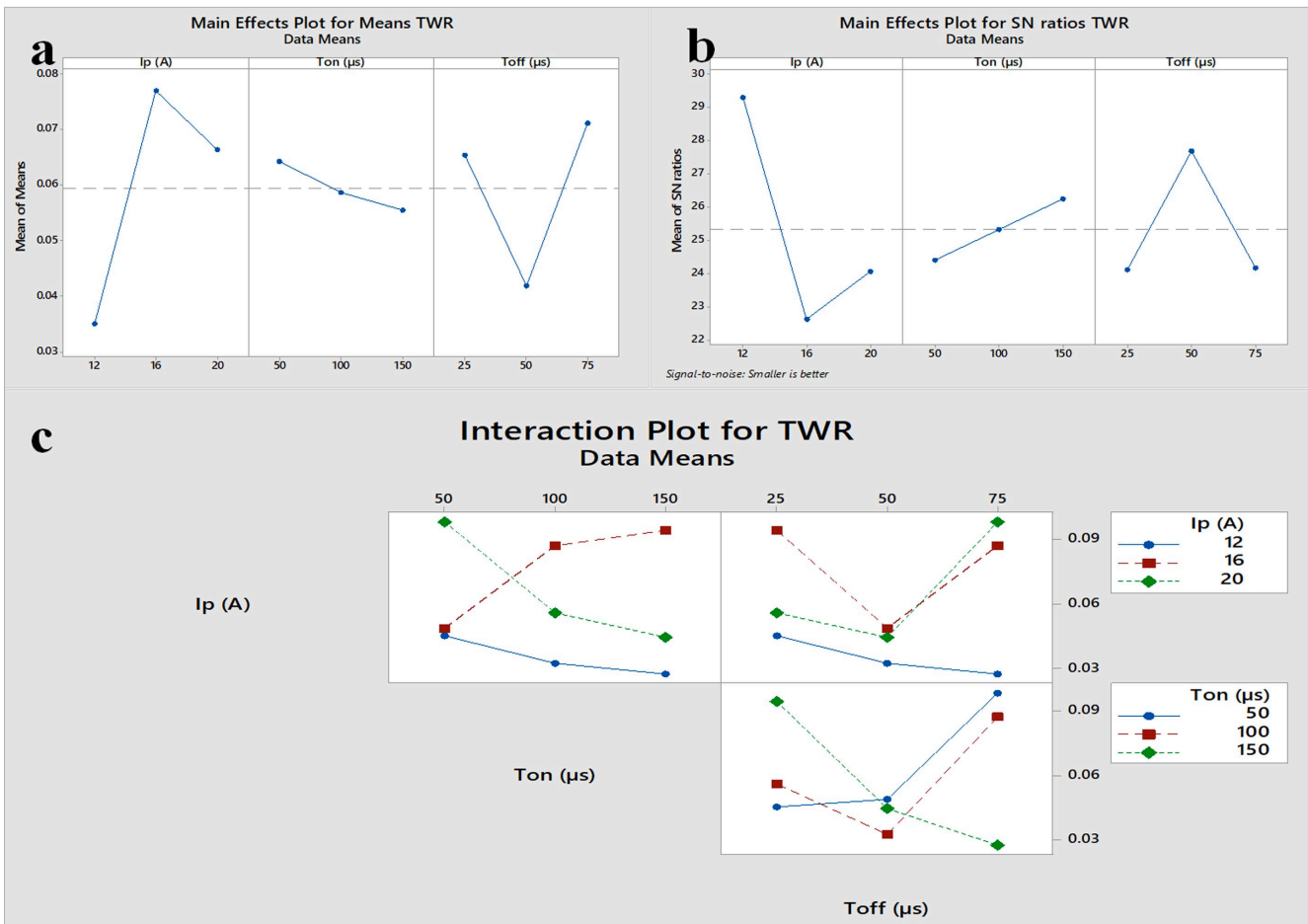


Fig. 5. (a) Main effects plot (Means) for TWR, (b) Main effects plot (Signal-to-Noise ratio) for TWR, (c) Interaction Plot for TWR Data Means

Fig. 5c illustrate interaction effect between input parameters on TWR. The minimum value of TWR is the better, it is achieved at (12A, 150  $\mu$ s and 75  $\mu$ s) of ( $I_p$ ,  $T_{on}$  and  $T_{off}$ ) respectively, that in level (1). As well as, lowest value of TWR is at (16 A, 50  $\mu$ s and 50  $\mu$ s) of ( $I_p$ ,  $T_{on}$  and  $T_{off}$ ) at level 2, and (20 A, 150  $\mu$ s and 50  $\mu$ s) of ( $I_p$ ,  $T_{on}$  and  $T_{off}$ ) in level 3. Furthermore, the interaction between  $I_p$ ,  $T_{on}$  and  $T_{off}$  for the lowest value of TWR is achieved at the less value of  $I_p$  and highest value of  $T_{on}$  and  $T_{off}$ , can see that in TABLE 2.

Fig. 6a, it can be seen decreases in the machining time (MT) with the increase of the  $I_p$  density and  $T_{on}$ . That, because the increase in erosion (melting and evaporation) with the increase discharge energy spark, which leads to a decrease of the MT [25]. As the  $T_{off}$  increases, the MT increases due to a slowdown in the erosion process due to the lack of discharge energy spark. Fig. 6b, can see the increase of MT in the beginning of operation, this is due to the instability of the operating process, then decreases due to the discharge energy, that lead to a decrease in MT with  $T_{off}$ . As described in the previous interaction plots, these plots give the appropriate value of inputs. Thus, appropriate value depends on the required value of outputs, if it required the highest value or the lowest.

Therefore, notice from Fig. 6b, that the highest values are at the  $I_p$ . This means that the  $I_p$  has a greater effect on the SN than  $T_{off}$  and  $T_{on}$ . A  $I_p$  value of 20 A has a greater effect than 16 A and 12 A. The same applies to the  $T_{on}$ , where, the highest level

(150  $\mu$ s) has the highest effect on SN ratio. But for  $T_{off}$  the effect is inverse, as the lowest value has the highest effect on noise, and vice versa. The higher values of SN ratio clear that control factor minimize the effect of the noise factors. Fig. 6c, described the interaction plot for time, it is clear at 20A of  $I_p$ , 100  $\mu$ s of  $T_{on}$  and 25  $\mu$ s of  $T_{off}$ , these gave the lower time. While from the interaction between  $T_{on}$  and  $T_{off}$  the lower value of time achieved at 100  $\mu$ s and 25  $\mu$ s of  $T_{on}$  and  $T_{off}$  respectively. This means that the variable with the highest delta will have the highest rank and vice versa. In other word, the peak current has three different values, which are 12, 16, and 20. TABLE 3 indicates that the mean response of outcomes, the rank of the effect of three input parameters on the outcomes depend on delta.

Delta is referring to the difference of the highest and the lowest value of the variables for the ranks of Minitab assigns, that based on delta values. While, rank refers to the order in which the three input parameters influence the results depends on the delta.

Therefore, it has three levels (1, 2, and 3), for example, level 1 has three attempts with a current value of 12, and so on for the rest of the variables. Thus, rank 1 for peak current, which have the highest delta value followed by a pulse-off time as rank 2 and pulse-on time rank 3.

TABLE 4 illustrated the contribution value for input parameters for 3 outputs. So, using a signal to noise (S/N) by analysis of variance (ANOVA), as statistical analysis to identify the signifi-

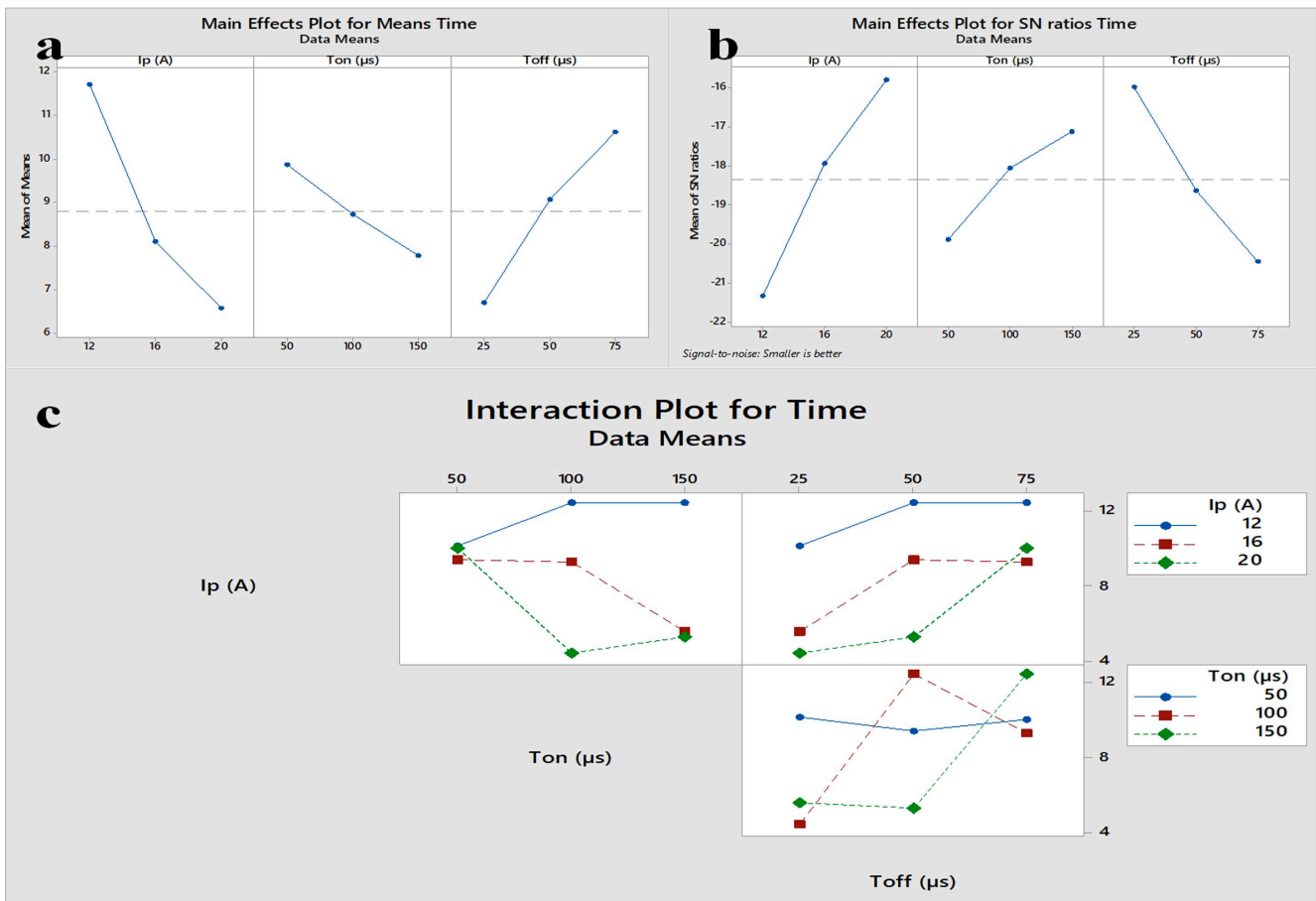


Fig. 6. (a) Main effects plot (Means) for Time, (b) Main effects plot (Signal-to-Noise ratio) for Time, (c) Interaction Plot for Time Data Means

Mean response table for outputs

Taguchi Analysis	Time			MRR			TWR		
	Mean response			Mean response			Mean response		
	$I_p$ (A)	$T_{on}$ ( $\mu$ s)	$T_{off}$ ( $\mu$ s)	$I_p$ (A)	$T_{on}$ ( $\mu$ s)	$T_{off}$ ( $\mu$ s)	$I_p$ (A)	$T_{on}$ ( $\mu$ s)	$T_{off}$ ( $\mu$ s)
Level 1	11.707	9.870	6.710	10.60	11.91	20.14	0.03510	0.06427	0.06540
Level 2	8.103	8.730	9.067	15.77	17.32	15.74	0.07700	0.05870	0.04193
Level 3	6.580	7.790	10.613	21.18	18.32	11.67	0.06640	0.05553	0.07117
Delta	5.127	2.080	3.903	10.58	6.41	8.46	0.04190	0.00873	0.02923
Rank	1	3	2	1	3	2	1	3	2

TABLE 4

ANOVA results for outputs

	Source	DF	SS	MS	Contribution	P-value
	<b>MRR of Sample</b> (mm <sup>3</sup> /min)	$I_p$ (A)	2	167.83	83.913	46.90%
$T_{on}$ ( $\mu$ s)		2	71.26	35.628	19.91%	0.134
$T_{off}$ ( $\mu$ s)		2	107.71	53.856	30.10%	0.093
Error		2	11.01	5.504	3.08%	
Total		8			100%	
<b>TWR of Tool</b> (mm <sup>3</sup> /min)		$I_p$ (A)	2	0.002848	0.001424	48.74%
	$T_{on}$ ( $\mu$ s)	2	0.000117	0.000059	2.01%	0.925
	$T_{off}$ ( $\mu$ s)	2	0.001439	0.000719	24.62%	0.500
	Error	2	0.001439	0.000720	24.63%	
	Total	8			100%	
	<b>Time (min)</b>	$I_p$ (A)	2	41.587	20.7936	56.86%
$T_{on}$ ( $\mu$ s)		2	6.510	3.2348	8.90%	0.222
$T_{off}$ ( $\mu$ s)		2	23.183	11.5910	31.69%	0.74
Error		2	1.862	0.9312	2.55%	
Total		8			100%	

cant factors and achieve the optimal value. The analysis achieved at 95% confidence level a significant level of (0.05) indicate as 5% risk. DF refer to the degree of freedom, and it depends on inputs and their level and it computed by the program itself after entering the value of each input with their level. After computed (DF) sum of the square of the variance (SS) and the mean sum of the square of the variance (MS) were computed. Therefore, sequence of influence referred to as a rank, and was using the contribution rate (P-value) in order to determine the percentage. As the rank sequence does not give the true value of the amount of influence. It only gives an impression of which factors are most influential and which are less influential. Therefore, percentage was used in order to clarify the amount of this influence.

The contributory value for each input was calculated depending on the degree of freedom of variables and the degree of freedom of error through ANOVA and it wrote down as a percentage value (P%). From table 4 for MRR and TWR,  $I_p$  also is the most effect factor with percentage values as 46.90% and 48.74% for MRR and TWR respectively.  $T_{on}$  have the lowest effect of TWR with contribution value as 2.01% lower than the error percentage value, so it can indicate as unaffected factor.

Also, for MT, it's obvious that  $I_p$  is the most effect factor in the percentage contribution value as 56.86% and it's followed by  $T_{off}$  and  $T_{on}$  as 31.69% and 8.90% respectively.

The core idea behind the Taguchi approach is to determine the unique and cumulative influence of design factors using the fewest possible experiments. The loss function is a reliable design technique that is used to qualify the performance departure from the desired outcome [26]. The three sorts of S/N ratios that are applicable are „larger is better“, „smaller is better“, and „nominal is better“, depending on the performance characteristic's purpose. Process parameter choices with the highest value of S/N ratio consistently produce the best quality with the least amount of volatility, regardless of the quality characteristic category [27]. Therefore, an optimal point must be obtained for EDM parameters, that can be obtained by statistical methods such as the Minitab program. That, is used to analyze the influence input parameters on output optimum value [28]. The increase of TWR with increasing of MRR at high current is normally, because the discharge energy per pulses is increased. Therefore, can be overcome this state by using dielectric fluid has low viscosity leads to good cleaning and cooling [29,30].

#### 4. Conclusion

In the current study, the appropriate examinations and electric discharge machining (EDM) are conducted to the composite material produced from aluminum alloy (Al5052) reinforced by Nano-aluminum oxide (Al<sub>2</sub>O<sub>3</sub>), where it can be list the following findings:

- The SEM examination before and after machining appear convergence between the images of aluminum alloy Al5052 and its composite. So, the SEM images was noted the stir casting method is suitable for aluminum matrix reinforced with ceramic materials. That, especially with small particle size, which as the homogenous structure was clear in the images. In addition, no cracks appeared on the samples surface after machining by electric discharge machining, which indicates that the mixing and distribution was good.
- The use hard ceramic particles as strengthening materials with the non-agglomeration and homogeneous distribution lead to refining the grain size and improve the hardness about 37.2%. Also, the composite hardness after machining is higher than the hardness of the composite before machining about 22.6%.
- The machining results of electrical discharge showed the material removal rate MRR and the tool wear rate TWR are affected directly by the peak current  $I_p$ . In other words, they are significantly increasing when the current is increased, and slightly increase with the  $T_{on}$  and  $T_{off}$ .
- The best design of input parameters ( $I_p$ ,  $T_{on}$  and  $T_{off}$ ) was (20 A, 100  $\mu$ s and 25  $\mu$ s) respectively, these values for (28.2904 mm<sup>3</sup>/min) of MRR outcome, with less time (4.40 min). While the best values of same input parameters were (16 A, 50  $\mu$ s and 75  $\mu$ s), respectively, for (0.0275 mm<sup>3</sup>/min) of TWR outcome.

#### REFERENCES

- [1] E.W.A. Fanani, E. Surojo, A.R. Prabowo, D. Ariawan, H. Ilham Akbar, Recent Development in Aluminum Matrix Composite Forging: Effect on the Mechanical and Physical Properties. *Procedia Structural Integrity* **33**, 3-10 (2021).
- [2] O. Muribwathoho, V. Msomi, S. Mabuwa, Metal Matrix Composite Fabricated with 5000 Series Marine Grades of Aluminium Using FSP Technique: State of the Art Review. *Appl. Sci.* **12**, 12832 (2022). DOI: <https://doi.org/10.3390/app122412832>
- [3] S. Capuzzi, G. Timelli, Preparation and Melting of Scrap in Aluminum Recycling: A Review. *Metals* **8**, 249 (2019). DOI: <https://doi.org/10.3390/met8040249>
- [4] K. Haikal, N.K. Yusuf, A. Hamdan, E. Nasha, Sustainable Aluminum Recycling Method. *Journal Of Multi-Disciplinary Engineering Reviews* **1**, 1, 8-19 (2024). DOI: <https://doi.org/10.30880/jmer.2024.01.01.002>
- [5] J. Singha, A. Chauhanb, Characterization of hybrid aluminum matrix composites for advanced applications – A review. *J. Mater. Res. Technol.* **5** (2), 159-169 (2015). DOI: <http://dx.doi.org/10.1016/j.jmrt.2015.05.004>
- [6] L. Singh, S. Kumar, S. Raj, P. Badhani, Aluminium metal matrix composites: manufacturing and applications. In: IOP conference series: materials science and engineering **1149**, 1, 012025 (2021). DOI: <https://doi.org/10.1088/1757-899X/1149/1/012025>
- [7] C. Saikrupa, G.C.M. Reddy, S. Venkatesh, Aluminium metal matrix composites and effect of reinforcements – A Review. *Materials Science and Engineering* **1057**, 1, 012098 (2021). DOI: <https://doi.org/10.1088/1757-899X/1057/1/012098>
- [8] A.Z. Ziva, Y.K. Suryana, Y.S. Kurniadianti, R. Ragadhita, A.B.D. Nandiyanto, T. Kurniawan, Recent Progress on the Production of Aluminum Oxide (Al<sub>2</sub>O<sub>3</sub>) Nanoparticles: A Review. *Mechanical Engineering for Society and Industry* **1**, 2, 54-77 (2021). DOI: <https://doi.org/10.31603/mesi.5493>
- [9] A.M. Rheima, Z.S. Abbas, M.M. Kadhim, S.H. Mohammed, D.Y. Alhameedi, F.A. Rasen, A.D.J. Al-Bayati, M. Ramadan, Z.T. Abed, A.S. Jaber, S. Hachim, F. K. Ali, Z.H. Mahmoud, E. Kianfar, Aluminum oxide nano porous: Synthesis, properties, and applications. *Case Studies in Chemical and Environmental Engineering* **8**, 100428 (2023). DOI: <https://doi.org/10.1016/j.cscee.2023.100428>
- [10] D. Wanwu, Y. Cheng, C. Taili, Z. Xiaoyan, L. Xiaoxiong, Research status and application prospect of aluminum matrix composites. *Research and Application of Materials Science* **2**, 1 (2020). DOI: <https://doi.org/10.33142/msra.v2i1.1975>
- [11] P.D. Srivyas, M. Charoo, Aluminum metal matrix composites a review of reinforcement; mechanical and tribological behavior. *International Journal of Engineering & Technology* **7**, 2.4, 117-122 (2018). Website: [www.sciencepubco.com/index.php/IJET](http://www.sciencepubco.com/index.php/IJET).
- [12] N. Kumbhar, S. Sahoo, I. Samajdar, G. Dey, K. Bhanumurthy, Microstructure and microtextural studies of friction stir welded aluminium alloy 5052. *Materials & Design* **32**, 3, 1657-1666 (2011). DOI: <https://doi.org/10.1016/j.matdes.2010.10.010>
- [13] A.A.H. Mahdy, A. Magdy, E. Mosa, A. Kandil, Effect of mwcnts on microstructure, dry sliding wear, and corrosion behavior of aa5052/mwcnts composite. *Journal of Al-Azhar University Engineering Sector* **16**, 61, 1212-1223 (2021).
- [14] J. Wu, F. Djavanroodi, M. Shamsborhan, S. Attarilar, M. Ebrahimi, Improving Mechanical and Corrosion Behavior of 5052 Aluminum Alloy Processed by Cyclic Extrusion Compression. *Metals* **12**, 8, 1288 (2022). DOI: <https://doi.org/10.3390/met12081288>
- [15] P. Samal, P.R. Vundavilli, Investigation of impact performance of aluminum metal matrix composites by stir casting. *IOP Conf. Series: Materials Science and Engineering* **653**, 012047 (2019). DOI: <https://doi.org/10.1088/1757-899X/653/1/012047>
- [16] M. Patel, S.K. Sahu, M.K. Singh, Fabrication and investigation of mechanical properties of SiC particulate reinforced AA5052 metal matrix composite. *Journal of Modern Materials* **7**, 1, 26-36 (2020). DOI: <https://doi.org/10.21467/jmm.7.1.26-36>

- [17] T. Mythili, R. Thanigaivelan, Optimization of wire EDM process parameters on Al6061/Al<sub>2</sub>O<sub>3</sub> composite and its surface integrity studies. *Bulletin of the Polish Academy of Sciences: Technical Sciences* **68**, 6 (2020).  
DOI: <https://doi.org/10.24425/bpasts.2020.135382>
- [18] A. Singha, K. Kumara, K.G. Sundarib, R. Ranjana, B. Surekhaa, Experimental investigations and multi criteria optimization during machining of A356/WC MMCs using EDM. *Decision Science Letters* **11**, 147-158 (2022).  
DOI: <https://doi.org/10.5267/dsl.2021.12.001>
- [19] H.S. Ram, M. Uthayakumar, S.S. Kumar, S.T. Kumaran, K. Korniejenko, Modelling Approach for the Prediction of Machinability in Al6061 Composites by Electrical Discharge Machining. *Appl. Sci.* **12**, 2673 (2022). DOI: <https://doi.org/10.3390/app12052673>
- [20] P.H.S. Masooth, G. Bharathiraja, V. Jayakumar, K. Palani, Analysis of machining characteristics in electrical discharge machining of SiC and Al<sub>2</sub>O<sub>3</sub> reinforced AA6061 hybrid metal matrix composites using Taguchi and ANOVA techniques, *Materials Research Express* **9**, 4, 046521 (2022).  
DOI: <https://doi.org/10.1088/2053-1591/ac672d>
- [21] C.O. Ujah, D.V.V. Kallon, Trends in aluminium matrix composite development. *Crystals* **12**, 10, 1357 (2022).  
DOI: <https://doi.org/10.3390/cryst12101357>
- [22] M. Dadkhah, A. Saboori, P. Fino, An overview of the recent developments in metal matrix nanocomposites reinforced by graphene. *Materials* **12**, 17, 2823 (2019).  
DOI: <https://doi.org/10.3390/ma12172823>
- [23] P. Sharma, S. Sharma, D. Khanduja, Production and some properties of Si<sub>3</sub>N<sub>4</sub> reinforced aluminium alloy composites. *Journal of Asian Ceramic Societies* **3**, 3, 352-359 (2015).  
DOI: <http://dx.doi.org/10.1016/j.jascer.2015.07.002>
- [24] C.G. Kuo, C.Y. Hsu, J.H. Chen, P.W. Lee, Discharge current effect on machining characteristics and mechanical properties of aluminum alloy 6061 workpiece produced by electric discharging machining process. *Advances in Mechanical Engineering* **9**, 11, (2017).  
DOI: <https://doi.org/10.1177/1687814017730756>
- [25] C. Kar, B. Surekha, H. Jena, S.D. Choudhury, Study of influence of process parameters in electric discharge machining of aluminum – red mud metal matrix composite. *Procedia Manufacturing* **20**, 392-399 (2018). [www.elsevier.com/locate/procedia](http://www.elsevier.com/locate/procedia).
- [26] R.K. Roy, Design of experiments using the Taguchi approach: 16 steps to product and process improvement. John Wiley & Sons (2001).
- [27] D. Hammami, S. Louati, N. Masmoudi, C. Bradai, Influence of WEDM process parameters on aluminum alloy's surface finish. *The International Journal of Advanced Manufacturing Technology* **126**, 1-2, 453-469 (2023).  
DOI: <https://doi.org/10.1007/s00170-023-10929-w>
- [28] K.Umanath, D.Devika, Optimization of electric discharge machining parameters on titanium alloy (ti-6al-4v) using Taguchi parametric design and genetic algorithm. *MATEC Web of Conferences* **172**, 04007 (2018).  
DOI: <https://doi.org/10.1051/mateconf/201817204007>
- [29] A.P. Markopoulos, E.L. Papazoglou, P.K. Obratański, Experimental study on the influence of machining conditions on the quality of electrical discharge machined surfaces of aluminum alloy Al5052. *Machines* **8**, 1, 12 (2020).  
DOI: <https://doi.org/10.3390/machines8010012>
- [30] A.S. Channi, H.S. Bains, J.S. Grewal, V.S. Chidamburanathan, R. Kumar, Tool wear rate during electrical discharge machining for aluminium metal matrix composite prepared by squeeze casting: A prospect as a biomaterial. *Journal of Electrochemical Science and Engineering* **13**, 1, 149-162 (2023).  
DOI: <https://dx.doi.org/10.5599/jese.1391>